JACS
JOURNAL OF THE AMERICAN CHEMICAL SOCIETY

COMMUNICATION

pubs.acs.org/JACS

Self-Assembly of Poly(ionic liquid)s: Polymerization, Mesostructure Formation, and Directional Alignment in One Step

Jiayin Yuan,*[,†] Sebastian Soll,[†] Markus Drechsler,[‡] Axel H. E. Müller,[‡] and Markus Antonietti[†]

[†]Department of Colloid Chemistry, Max Planck Institute of Colloids and Interfaces, D-14476 Potsdam, Germany

[‡]Macromolecular Chemistry II, University of Bayreuth, D-95440 Bayreuth, Germany

Supporting Information

ABSTRACT: This paper reports on the highly ordered and tunable inner structure of poly(ionic liquid) nanoparticles, which formed spontaneously by precipitation polymerization from water. Without added stabilizer, these "latexes" are much smaller (20−40 nm in diameter) than usual polymer latexes and exhibit either multilamellar or unilamellar vesicular morphology, depending on the tail length of the quaternizing alkyl chains. The simplicity in the synthesis and composition and the high complexity of the ordered structures that resemble liposomes expand the classical profile of homopolymer self-assembly. In addition, unidirectional superassembly to a nanoworm mesostructure is found at elevated concentrations, indicating that the ionic liquid liposomes are apt to integrate into further hierarchical assembly schemes.

Polymeric nanoparticles combine the benefits of nanoparticles (such as high surface-to-volume ratio) with the superior processability, flexibility of functionality, and price/scale-up possibilities of polymers. Apart from their interest in fundamental research, they have already found a multitude of applications in the fields of biotechnology, sensing, separation and purification, etc.[1−5] A number of synthetic approaches and processing techniques can be employed for the preparation of polymeric nanoparticles, including emulsion, suspension and dispersion−precipitation polymerization, miniemulsion processes, block copolymer self-assembly, intramolecular cross-linking routes, solvent evaporation exchange methods, and many more.[6−15] Each of these methods and techniques governs different aspects of the nanoparticles, among which dimension, morphology (sphere, rod, wire, etc.), surface functionality, chemical composition, and inner structures are the major ones that determine their properties and functions. So far, most efforts have been devoted to controlling the dimension, outside morphology, chemical composition, and surface functionality within the synthesis.

On the other hand, the preparation of polymer nanoparticles with well-defined inner structures has been more rarely reported. Via a miniemulsion process, Landfester et al. and Heroguez et al. demonstrated the synthesis of biphasic polymer nanoparticles formed from two immiscible polymers;[16,17] a self-organized precipitation method was employed by Higuchi et al. to prepare polymer nanoparticles with inner microphase separation.[18] There has also been some work on block copolymer nanoparticles in water,[19] by simple solvent exchange from a prepolymerized block copolymer[20] or by interpolyelectrolyte complex formation.[21] In addition to being beautiful and an object of basic research, such internally structured polymer nanoparticles have plenty of potential applications. For instance, polymer nanoparticles having two different nanocompartments with different solubility behavior can be used for advanced drug delivery applications,[22−24] for dissolving/removing substrates with very different polarities, or as structured catalysis supports.[20,25]

Meanwhile, poly(ionic liquid)s (PILs) have attracted considerable attention recently, because they combine some unique characters of ionic liquids with the common properties of polymers, such as processability, durability, mechanical stability, etc. This makes PILs a class of versatile polymers for a multitude of applications, for instance solid ion conductors, CO_2 sorbents, dispersants, porous materias, carbon precursors, etc.[26−28] The self-assembly of PILs has received special interest due to its potential application as nanostructured functional materials.[26,27,29] More recently, we have introduced a facile method to prepare PIL nanoparticles via dispersion polymerization of vinylimidazolium-type ionic liquid monomers (ILMs) with long alkyl chains. The polymerization proceeded over 24 h at a monomer concentration of 50 g/L in aqueous solutions at 70 °C using the water-soluble nonionic initiator 2,2′-azobis[2-methyl-*N*-(2-hydroxyethyl)propionamide] (VA86).[30] It required no externally added stabilizer, as the ILMs and their oligomers could act as effective dispersants.[31,32] It was assumed, although not experimentally proven, that the as-formed PIL nanoparticles were most likely setup in organized mesophases made up from separated nanodomains of the charged IL moieties and the long hydrophobic alkyl chains. This would follow similar organization patterns found in polyelectrolyte−surfactant complexes[33−35] or in alkyl-substituted rigid-rod polymers, which is driven by the incompatibility of alkyl tails with many polar polymeric backbones.[36−38] In the present contribution, we report on our further research efforts on PIL nanoparticles which revealed that these nanoparticles exhibit highly ordered and tunable concentric multi- or unilamellar inner structures. This structure formed spontaneously throughout polymerization in a single step. This simultaneous and cooperative process is rather unique.

The PIL nanoparticles were prepared from the ILMs 3-*n*-dodecyl-1-vinylimidazolium bromide (ILM-C12) and the corresponding C14−C18 derivatives (ILM-C14, ILM-C16, and ILM-C18). They are named poly(ILM-C12), poly(ILM-C14), poly(ILM-C16), and poly(ILM-C18) (chemical structures in Scheme 1). Their average sizes, as determined by dynamic light

Received: July 28, 2011
Published: October 07, 2011

Scheme 1. Chemical Structures of Poly(ionic liquid) Nanoparticles of poly(ILM-C12), poly(ILM-C14), poly(ILM-C16), and poly(ILM-C18)

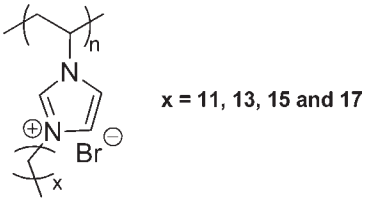

scattering (DLS), are 30, 34, 35, and 39 nm, while the standard size deviation of these nanoparticles is in the range of 0.4−0.6. Already the special shape of the particle size distribution points to the presence of a unique organization effect, as will be discussed below. The nanoparticle dispersions are colloidally stable, but after complete drying, film formation toward an organized film takes place, which is no longer redispersible.

Room-temperature transmission electron microscopy (TEM) images of these four PIL nanoparticles are presented in Figure S1 (Supporting Information). Due to a drying effect, the inner nanostructure of the PIL nanoparticles was hard to recognize, which is presumably due to structure reorganization toward a homogenic orientation: i.e., parallel to the film surface. To access the true structure, cryogenic TEM (cryo-TEM) measurements were performed by shock-freezing a thin film (∼100 nm) of the aqueous nanoparticle suspensions at room temperature (20 °C) on lacey TEM grids.

Parts A−K of Figure 1 display the cryo-TEM images taken from aqueous solutions of poly(ILM-C12), poly(ILM-C14), poly(ILM-C16), and poly(ILM-C18) nanoparticles. Onionlike multilamellar vesicular nanostructures are clearly visible in the samples of poly(ILM-C12) (Figure 1A) and poly(ILM-C14) (Figure 1C) nanoparticles, while a lipid-like unilamellar vesicular morphology is dominant in the samples of poly(ILM-C16) (Figure 1E) and poly(ILM-C18) (Figure 1G) nanoparticles. In Figure 1A, the poly(ILM-C12) nanoparticles are quasi-spherical in shape. In spite of the size variation of the nanoparticles, the onionlike inner nanostructure is exclusively observed. A close view of these nanoparticles is given in Figure 1B. The multilamellar character is clearly visible, and the number of bilayers can be easily counted. A statistical calculation reveals that the nanoparticle size is distinct in steps and is simply controlled by the number of bilayers. Apparently, larger nanoparticles have more layers in the onionlike structures than in the smaller ones. The distance between layers is calculated by fast Fourier transform (FFT) from such pictures. An average value of 3.42 nm was obtained for the poly(ILM-C12) nanoparticles.

Similar multilamellar vesicles were observed in the cryo-TEM image of poly(ILM-C14) nanoparticles (Figure 1C). However, in comparison to Figure 1A, it is easily seen that the poly(ILM-C14) nanoparticles possess a number of bilayers smaller than that of poly(ILM-C12). The average distance between layers calculated from FFT is 3.78 nm, which is about 0.36 nm larger than that of the poly(ILM-C12) nanoparticles. As the full length of one $-(CH_2CH_2)-$ unit is 0.254 nm, this clearly points to a slightly tilted or disordered bilayer structure.[33,37] In addition, a central "void" is spontaneously formed, whose size is somehow independent of the bilayer number. This is clearly attributed to the maximum spontaneous bendability of the layers, which is less for longer alkyl tails.

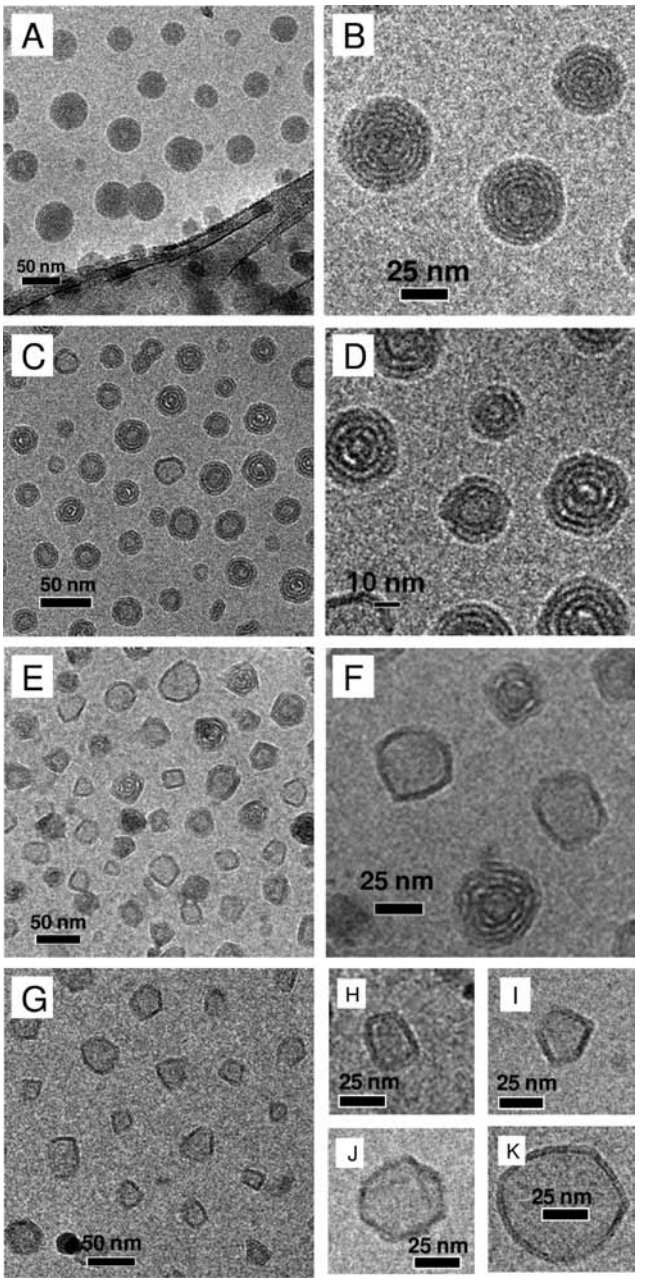

Figure 1. Representative cryo-TEM images of PIL nanoparticles in aqueous solution: (A, B) poly(ILM-C12); (C, D) poly(ILM-C14); (E, F) poly(ILM-C16); (G−K) poly(ILM-C18).

When the alkyl chain length is increased from C14 to C16, the central "void" expands its dimension. Following this change, two distinct effects can be observed for poly(ILM-C16) nanoparticles. (a) A lipidlike unilamellar structure coexists with onionlike multilamellar nanoparticles. The former is in fact dominant (>60%). The size of poly(ILM-C16) particles (35 nm) determined from DLS remains similar to that of poly(ILM-C14) particles (34 nm). The volume expansion by the central "void" is thus compensated by a reduced number of bilayers. (b) Instead of a near-spherical morphology, poly(ILM-C16) nanoparticles show an anisotropic rigid shape, for instance, rectangles or pentagons, as illustrated in higher magnification in Figure 1F. These effects become more pronounced when the alkyl chain

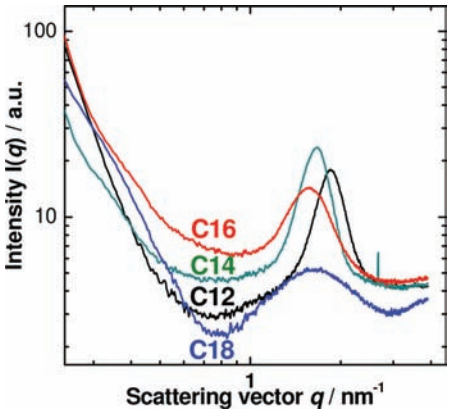

Figure 2. Small-angle X-ray scattering patterns of aqueous dispersions of PIL nanoparticles.

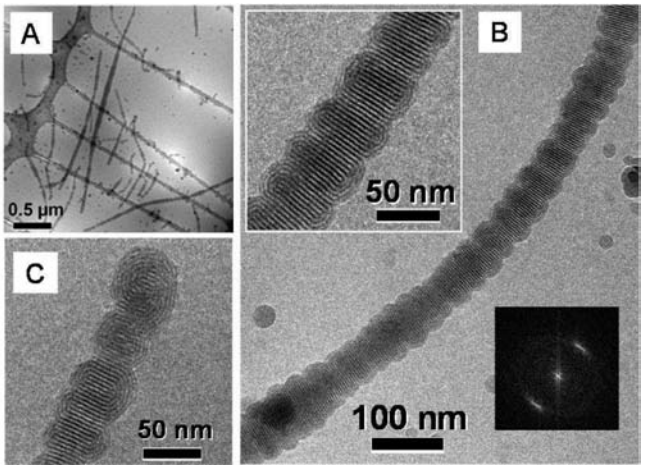

Figure 3. cryo-TEM images of nanoworm superstructures of poly(ILM-C12) prepared at monomer concentration of 100 g/L: (A) overview; (B) close view of a single nanoworm; (C) tail structure of the nanoworm. The top inset in (B) is an enlarged view, and the bottom inset is the corresponding FFT pattern.

length is increased to C18. As shown in Figure 1G, the poly(ILM-C18) nanoparticles exhibit exclusively a unilamellar structure with well-defined geometry, such as rectangles (Figure 1H), pentagons (Figure 1I), hexagons (Figure 1J), and even polyhedrons (Figure 1K). The formation of these anisotropic nanoparticles is believed to be due to the development of side-chain crystallinity in the alkyl phase. Differential scanning calorimetry measurements (Figure S3 (Supporting Information)) of dried PIL samples (−50 to 150 °C) show that poly(ILM-C12) is amorphous, while the alkyl chains in poly(ILM-C14), poly(ILM-C16), and poly(ILM-C18) crystallize at 1, 21, and 35 °C, respectively. Samples for cryo-TEM experiments were prepared at 20 °C, at which poly(ILM-C16) is partially crystalline and poly(ILM-C18) is predominantly crystalline. This explains the distinct shape of poly(ILM-C16) and poly(ILM-C18), as crystalline structures are often responsible for various nanoobjects with defined folds. In general, cryo-TEM characterization evidently reveals that, from poly(ILM-C12) to poly(ILM-C18), there is an obvious transition in the inner structures from onionlike multilamellar to unilamellar vesicles, though less variation in the overall size is observed.

To receive a complementary view of the inner structure of PIL nanoparticles, small-angle X-ray scattering (SAXS) measurements of the PIL nanoparticle dispersions were performed at a concentration of 50 g/L. As shown in Figure 2, the SAXS pattern clearly shows a primary q value, which corresponds to d spacings of 3.40, 3.80, 4.00, and 3.90 nm for poly(ILM-C12), poly(ILM-C14), poly(ILM-C16), and poly(ILM-C18), respectively. The d spacings of poly(ILM-C12) and poly(ILM-C14) determined from SAXS patterns and cryo-TEM images (3.42 and 3.78 nm) are in good accord. It has been reported that polyelectrolyte−surfactant complexes or rigid-rod-like polymers with long alkyl chains (>C8) form layered mesophases, whose d spacing increases linearly with the alkyl chain length.[36,37,39] In our case, the d spacing increases nonlinearly from C12 to C16 and decreases at C18. This can be related to the onset of crystallization from C14 to C18, as already indicated in cryo-TEM characterization. In the SAXS pattern of poly(ILM-C16) the onset of the second peak occurs at the highest q value illustrated (Figure 2), and it becomes more obvious in poly(ILM-C18). The X-ray diffraction patterns of the solid PIL powders (Figure S4 (Supporting Information)) provide further hints. While poly(ILM-C12) and poly(ILM-C14) are in an amorphous state with respect to the side chains, poly(ILM-C18) presents clear peaks that can be indexed to a tetragonal arrangement, presumably regular undulations which further limit the bendability of the layers.[20] The d spacing decreases from PIL-C16 to PIL-C18, as the crystallization promotes interdigitated packing.

It should be mentioned that these ordered nanoparticle structures formed during polymerization: i.e., polymer chain formation and self-assembly take place in one step. cryo-TEM (Figure S5 (Supporting Information)) as well as dynamic light scattering measurements of the monomer solution under polymerization conditions revealed that the solution contained only small ILM micelles of ∼7 nm in diameter; thus, the nanoparticles have to be nucleated from this stage. We assume that the particles nucleate from the first formed polymers, analogous to the general models of microemulsion polymerization. These primary particles then swell with monomer to stabilize themselves into closed shells. The PIL nanoparticles with well-defined inner shell structures therefore stem from a unique simultaneous polymerization/self-assembly process. Note that we did not find any particles with incomplete shells, that is, polymerization takes place in the perfected structure, while exchange between the particles and structural improvement stems from the exchange of monomers being soluble in the continuous phase water.

In the cryo-TEM characterization, all PIL nanoparticles were observed as individual objects when prepared. However, at higher polymerization concentrations (100 g/L), the crystalline poly(ILM-C16) and poly(ILM-C18) remain nanoparticles, while in the amorphous poly(ILM-C14) elongated superstructures start to appear. In poly(ILM-C12), this structure evolution is the most pronounced. Figure 3A shows an overview of the nanoworms. Their size is in the range of micrometers, and some can be even longer than 100 μm: i.e., consisting of several hundreds of nanoparticles linearly connected. Figure 3B offers a close view of a single nanoworm. The nanoworm is in fact a string of nanoparticles, in which the concentric lamellae are reorganized to achieve an extended internanoparticle multilamellar conformation. The inset illustrates that the central lamellae exist in a fairly parallel fashion, while the contour partially maintains the structure of individual nanoparticles. The tail of the nanoworm, usually considered as a "defect" tethered to the end of the one-dimensional

nanostructure, is displayed in Figure 3C. As clearly observed, the terminal unit resembles still a "normal" nanoparticle with only slight deformation, while after one more unit the parallel lamella is perfectly developed. Such directional assembly or vectorial organization is well-known from biomineralization or mesocrystals,[40,41] but is—to the best of our knowledge—unseen in the polymer or soft matter nanostructure. The liquid character of the interior seems to be mandatory in the present case, which is understandable, as the particles have to deform to create the apparently optimal parallel alignment of the inner layers. It must be said that the strongest Hamaker forces are obtained by charge polarization when the polarization direction is parallel to the surface,[42] making charge and mirror charge formation the most simple and the nearest. The mechanism is obviously nicely observed in the present pictures. Note that mirror charge formation requires a liquid ionic state, which excluded the crystalline C16 and C18 particles from this alignment mechanism.

In conclusion, we have presented here the analysis of the inner structure of PIL nanoparticles, which already as a homopolymer are highly ordered and can be tuned from multilamellar to unilamellar vesicles, depending on the length scale of the alkyl chains. The polymers spontaneously self-assembled into mesostructures during polymerization. At higher concentrations, a novel 1D superstructure of nanoparticles with extended multilamellar substructure is found. With this unique example, we show that complex and hierarchically structured polymer assemblies can be formed by polymeric ionic liquids along a simple synthetic pathway.

■ ASSOCIATED CONTENT

Supporting Information. Text and figures giving experimental details and additional characterization data for the PIL nanoparticles. This material is available free of charge via the Internet at http://pubs.acs.org.

■ AUTHOR INFORMATION

Corresponding Author

*E-mail: Jiayin.yuan@mpikg.mpg.de. Fax: 49-331-5679502. Tel: 49-331-5679552.

■ ACKNOWLEDGMENT

This research was financially supported by the Max Planck Society. We acknowledge Dr. J. Weber and Dr. K. Tauer for helpful discussions.

■ REFERENCES

(1) Ambrosi, A.; Morrin, A.; Smyth, M. R.; Killard, A. J. *Anal. Chim. Acta* **2008**, *609*, 37–43.
(2) Cayre, O. J.; Chagneux, N.; Biggs, S. *Soft Matter* **2011**, *7*, 2211–2234.
(3) Bae, Y.; Fukushima, S.; Harada, A.; Kataoka, K. *Angew. Chem., Int. Ed.* **2003**, *42*, 4640–4643.
(4) Di, C.; Jiang, X.; Wang, R.; Yin, J. *J. Mater. Chem.* **2011**, *21*, 4416–4423.
(5) Hoshino, Y.; Haberaecker Iii, W. W.; Kodama, T.; Zeng, Z.; Okahata, Y.; Shea, K. J. *J. Am. Chem. Soc.* **2010**, *132*, 13648–13650.
(6) Li, B.; Huang, X.; Liang, L.; Tan, B. *J. Mater. Chem.* **2011**, *20*, 7444–7450.
(7) Kietzke, T.; Neher, D.; Landfester, K.; Montenegro, R.; Guntner, R.; Scherf, U. *Nat. Mater.* **2003**, *2*, 408–412.
(8) Walther, A.; Müller, A. H. E. *Soft Matter* **2008**, *4*, 663–668.
(9) Tauer, K.; Weber, N.; Texter, J. *Chem. Commun.* **2009**, 6065–6067.
(10) Oh, J. K.; Tang, C.; Gao, H.; Tsarevsky, N. V.; Matyjaszewski, K. *J. Am. Chem. Soc.* **2006**, *128*, 5578–5584.
(11) Liang, G.; Xu, J.; Wang, X. *J. Am. Chem. Soc.* **2009**, *131*, 5378–5379.
(12) Cherian, A. E.; Sun, F. C.; Sheiko, S. S.; Coates, G. W. *J. Am. Chem. Soc.* **2007**, *129*, 11350–11351.
(13) Foster, E. J.; Berda, E. B.; Meijer, E. W. *J. Am. Chem. Soc.* **2009**, *131*, 6964–6966.
(14) Nguyen, M. N.; Mougnier, S.-J.; Ibarboure, E.; Heroguez, V. *J. Polym. Sci., Part A: Polym. Chem.* **2010**, *49*, 1471–1482.
(15) Yan, F.; Texter, J. *Chem. Commun.* **2006**, 2696–2698.
(16) Kietzke, T.; Neher, D.; Kumke, M.; Ghazy, O.; Ziener, U.; Landfester, K. *Small* **2007**, *3*, 1041–1048.
(17) Airaud, C.; Heroguez, V.; Gnanou, Y. *Macromolecules* **2008**, *41*, 3015–3022.
(18) Higuchi, T.; Tajima, A.; Yabu, H.; Shimomura, M. *Soft Matter* **2008**, *4*, 1302–1305.
(19) Wei, R.; Luo, Y.; Li, Z. *Polymer* **2011**, *51*, 3879–3886.
(20) Kim, B.-S.; Taton, T. A. *Langmuir* **2006**, *23*, 2198–2202.
(21) Schacher, F.; Betthausen, E.; Walther, A.; Schmalz, H.; Pergushov, D. V.; Müller, A. H. E. *ACS Nano* **2009**, *3*, 2095–2102.
(22) Shim, J.; Seok Kang, H.; Park, W.-S.; Han, S.-H.; Kim, J.; Chang, I.-S. *J. Controlled Release* **2004**, *97*, 477–484.
(23) Riley, T.; Govender, T.; Stolnik, S.; Xiong, C. D.; Garnett, M. C.; Illum, L.; Davis, S. S. *Colloids Surf., B* **1999**, *16*, 147–159.
(24) Jeong, Y.-I.; Cheon, J.-B.; Kim, S.-H.; Nah, J.-W.; Lee, Y.-M.; Sung, Y.-K.; Akaike, T.; Cho, C.-S. *J. Controlled Release* **1998**, *51*, 169–178.
(25) Lu, Z.; Liu, G.; Phillips, H.; Hill, J. M.; Chang, J.; Kydd, R. A. *Nano Lett.* **2001**, *1*, 683–687.
(26) David, M. *Prog. Polym. Sci.* **2011**, DOI:10.1016/j.progpolymsci.2011.05.007.
(27) Green, O.; Grubjesic, S.; Lee, S.; Firestone, M. A. *Polym. Rev.* **2009**, *49*, 339–360.
(28) Lu, J.; Yan, F.; Texter, J. *Prog. Polym. Sci.* **2009**, *34*, 431–448.
(29) Grubjesic, S.; Seifert, S. n.; Firestone, M. A. *Macromolecules* **2009**, *42*, 5461–5470.
(30) Yuan, J.; Antonietti, M. *Macromolecules* **2011**, *44*, 744–750.
(31) Ma, X.; Crombez, R.; Ashaduzzaman, M.; Kunitake, M.; Slater, L.; Mourey, T.; Texter, J. *Chem. Commun.* **2011**, *47*, 10356–10358.
(32) Ma, X.; Ashaduzzaman, M.; Kunitake, M.; Crombez, R.; Texter, J.; Slater, L.; Mourey, T. *Langmuir* **2011**, *27*, 7148–7157.
(33) Antonietti, M.; Maskos, M. *Macromolecules* **1996**, *29*, 4199–4205.
(34) Antonietti, M.; Burger, C.; Thunemann, A. *Trends Polym. Sci.* **1997**, *5*, 262–267.
(35) Antonietti, M.; Radloff, D.; Wiesner, U.; Spiess, H. W. *Macromol. Chem. Phys.* **1996**, *197*, 2713–2727.
(36) Ballauff, M.; Schmidt, G. F. *Makromol. Chem., Rapid Commun.* **1987**, *8*, 93–97.
(37) Ballauff, M.; Schmidt, G. F. *Mol. Cryst. Liq. Cryst.* **1987**, *147*, 163–&.
(38) Holm, C.; Rehahn, M.; Oppermann, W.; Ballauff, M. In *Polyelectrolytes with Defined Molecular Architecture II*; Springer-Verlag: Berlin, 2004; Vol. 166, pp 1−27.
(39) Thünemann, A. F. *Prog. Polym. Sci.* **2002**, *27*, 1473–1572.
(40) Cölfen, H.; Mann, S. *Angew. Chem., Int. Ed.* **2003**, *42*, 2350–2365.
(41) Cölfen, H.; Antonietti, M. *Angew. Chem., Int. Ed.* **2005**, *44*, 5576–5591.
(42) Taden, A.; Landfester, K.; Antonietti, M. *Langmuir* **2004**, *20*, 957–961.